Ferromagnetic Josephson junctions with steplike interface transparency

N. G. Pugach,[1,*] M. Yu. Kupriyanov,[2] A. V. Vedyayev,[1] C. Lacroix,[3] E. Goldobin,[4] D. Koelle,[4] R. Kleiner,[4] and A. S. Sidorenko[5,6]

[1]*Faculty of Physics, M.V. Lomonosov Moscow State University, 119992 Leninskie Gory, Moscow, Russia*

[2]*Nuclear Physics Institute, M.V. Lomonosov Moscow State University, 119992 Leninskie Gory, Moscow, Russia*

[3]*Institut Néel, CNRS–UJF, BP 166, 38042 Grenoble Cedex 9, France*

[4]*Physikalisches Institut–Experimentalphysik II and Center for Collective Quantum Phenomena, Universität Tübingen, Auf der Morgenstelle 14, D-72076 Tübingen, Germany*

[5]*Institute of Electronic Engineering and Industrial Technologies, ASM, MD2028 Kishinev, Moldova*

[6]*Institute of Nanotechnology, Karlsruhe Institute of Technology (KIT), D-76021 Karlsruhe, Germany*

(Received 19 June 2009; published 20 October 2009)

Within the framework of the quasiclassical Usadel equations we study the Josephson effect in superconductor-insulator-ferromagnet-superconductor (SIFS) and SIFNS (N is a normal metal) structures with a steplike transparency of the FS or NS interface. At certain parameters the steplike transparency leads to the formation of a region, where the critical current-density distribution $J_C(y)$ along the junction exhibits a damped oscillation with a sign change. This results in the formation of a 0-π nanojunction with the characteristic length of 0 and π regions of the order of the coherence length ξ_F for SIFS and ξ_N for SIFNS junctions, respectively. Using several transparency steps one can create an array of nanojunctions. Such structures exhibit an unusual behavior in an external magnetic field H. The total critical current grows with increasing H up to a certain value, which depends on the size of a single nanojunction, and has multiperiodic oscillations in the case of an array.

DOI: 10.1103/PhysRevB.80.134516 PACS number(s): 74.45.+c, 74.50.+r, 74.78.Fk

I. INTRODUCTION

Recently, unconventional properties of Josephson junctions (JJs) have attracted a lot of attention.[1–3] Contrary to the already well-known 0 JJs with a Josephson phase $\varphi=0$ in the ground state, junctions with ferromagnetic barriers may have a ground state with $\varphi=\pi$ (π-JJs). These junctions may be used in electronic circuits, e.g., in JJ flux qubits with low decoherence,[4] self-biased rapid single flux quantum digital circuits,[5] or complementary logic.[6] If the current-phase relation of a JJ has the usual form $J(\varphi)=J_C\sin(\varphi)$ the ground state $\varphi=0$ is realized for $J_C>0$ and the ground state $\varphi=\pi$ for $J_C<0$. The last condition may be satisfied in the case of a ferromagnetic barrier. Such a junction consists of two superconducting electrodes (S) separated by the ferromagnetic layer (F). It could include also a thin insulating tunnel barrier (I), i.e., SFS or SIFS multilayers may be considered.

Modern technology allows to manufacture not only 0 or π-JJs but also the so-called 0-π Josephson junctions, i.e., junctions some parts of which behave as 0 junctions and other parts behave as π junctions.[7] In these structures, intensively studied experimentally, the different sign of J_C can be achieved by introducing a steplike change in the thickness of the F layer.[8–12]

The interest in these structures has been stimulated by the existence of unusual topological vortex solutions in these 0-π junctions. A spontaneous Josephson vortex carrying a fraction of the magnetic-flux quantum $\Phi_0\approx 2.07\times 10^{-15}$ Wb may appear at a 0-π boundary.[7,13,14] In the region, where the phase φ changes from 0 to π, there is a nonzero gradient $\partial\varphi/\partial y$ of the Josephson phase along the junction that is proportional to the local magnetic field. In essence this field is created by supercurrents $\sim\sin(\varphi)$ circulating in this region. These currents are localized in a λ_J vicinity of the 0-π boundary (λ_J is the Josephson penetration depth) and create a vortex of supercurrent with total magnetic flux equal to $\pm\Phi_0/2$, whereas a usual Josephson vortex carries $\pm\Phi_0$, provided that the junction length $L\gg\lambda_J$. In the case of $L\lesssim\lambda_J$ the spontaneous flux[7,13,15–17] $|\Phi|<\Phi_0/2$. It was shown theoretically[17,18] and indicated in experiments[9–11] that for certain conditions the existence of a fractional Josephson vortex at the 0-π boundary is energetically favorable in the ground state. The fractional vortex is pinned at the 0-π boundary and has two polarities that may be used for information storage and processing in the classical and quantum domains, e.g., to build JJ-based qubits.[19] We note that the fractional vortex described above is always pinned and is different from fractional Josephson vortices that are the solutions of a double sine-Gordon equation.[20–22]

Not only single Josephson junctions but also superconducting loops intersected by two JJs [dc superconducting quantum interference devices (SQUIDs)] and their arrays may be used in applications. Such arrays consist of N Josephson junctions connected as a one-dimensional parallel chain in such a way that $N-1$ individual superconducting loops are formed. Such an array exhibits an unusual dependence of its mean voltage on the magnetic field H for overcritical applied bias current. If the loops are identical the voltage response $V(H)$ is Φ_0 periodic. For JJ arrays with incommensurate loop areas the voltage response $V(H)$ is nonperiodic, and can have a rather sharp dip at $H=0$. This property may be used to create a sensitive absolute field magnetometer that is called superconducting quantum interference filter (SQIF).[23–27] So far, these SQIFs are based on usual JJs. However, recently it was also suggested to realize 0-π SQIFs, using constriction junctions in d-wave superconductors.[28] In the present paper we suggest SQIF-like

structures of a distinct type based on 0-π *s*-wave JJs with a ferromagnetic barrier.

In many investigations of 0-π JJs, it is assumed that the length of the junction $L \gg \lambda_J$ and that the critical current density is uniform along every part of the junction. The peculiarities arising on the nanoscale in the vicinity of the 0-π boundaries are usually neglected. In this work we show in the framework of a microscopic theory of superconductivity that if some property of the JJ changes in a stepwise manner, its critical current density J_C may have a peculiar oscillatory dependence in the vicinity of the step. This leads to an unusual dependence of the maximum supercurrent $I_{\max}(H)$ vs the external magnetic field. Instead of the Fraunhofer pattern usually observed for a uniform JJ, $I_{\max}$ grows linearly with H on a comparatively large interval. This behavior can be realized for certain junction parameters, e.g., for specific values of the ferromagnetic layer thickness d_F. We have obtained this result for SIFS JJs assuming the existence of a steplike nonuniformity in the transparency of the FS boundary, which should be sharp on the scale of the ferromagnetic coherence length ξ_F.[29] The practical realization of this structure may be difficult as the typical value of $\xi_F \sim 1$ nm. One of the possible solutions is to introduce a normal metal (N) into the junction, i.e., to use a SIFNS structure. Then, the relevant length is $\xi_N \sim 100$ nm $\gg \xi_F$, as a consequence of the proximity effect between F and N layers. Fabrication of such steps should not pose technological problems. The next step would be to make an array of these junctions, e.g., as in SQIFs.

This paper is organized as follows. In Sec. II we describe the model based on the linearized Usadel equation for a SIFS junction with a steplike transparency of the FS boundary. Its behavior in an external magnetic field is investigated. Sec. III describes SIFNS structures with a steplike transparency of the NS boundary. The properties of asymmetric SIFNS junctions with few different steps of the boundary transparency are presented in Sec. IV. In Sec. V the magnetic properties of symmetric and asymmetric periodic arrays of these junctions are described. Section VI concludes this work. The calculation details can be found in the Appendix.

II. MODEL FOR SIFS JUNCTION

A. Critical current-density distribution

We consider a Josephson junction of length L consisting of two semi-infinite superconducting electrodes separated by a ferromagnetic layer of thickness d_F and a thin insulating film of thickness d_I, $d_I \ll d_F$ (see Fig. 1).

The IF interface coincides with the yz plane, and it is assumed that the structure is homogeneous in the z direction but not in the y direction. The suppression parameters γ_{B1} and γ_{B2} for the parts of the FS interface located at $0 \le y \le L/2$ and $L/2 \le y \le L$, respectively, are supposed to be large enough to neglect the suppression of superconductivity in the S part of the SF proximity system in the structure. $\gamma_{B1(2)} = R_{B1(2)} S / 2\rho_F \xi_F$, where $R_{B1(2)}$ is the resistance of the corresponding part of the FS interface, S is the area of the junction, and ρ_F is the F metal resistivity. We assume that the dirty limit condition $l \ll \xi_{F,N,S}$ is fulfilled in the F and S layers

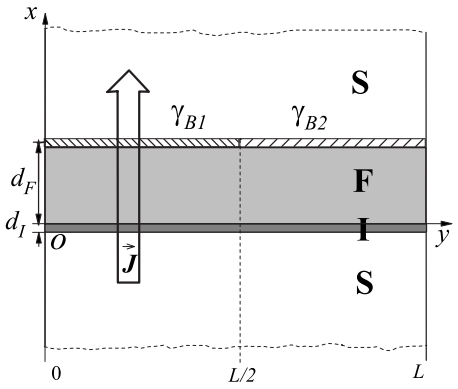

FIG. 1. Schematic view of the SIFS Josephson junction with a steplike change in the FS interface transparency ($\gamma_{B1} \neq \gamma_{B2}$).

and that the effective electron-phonon coupling constant is zero in the F metal.

Let either be the temperature T close to the critical temperature T_c of the superconducting electrodes or the suppression parameters at the FS interface large enough ($\gamma_{B1}, \gamma_{B2} \gg 1$) to permit the use of the linearized Usadel equations in the F film. Under the above restrictions the problem of calculation of the critical current density in the structure reduces to the solution of the two-dimensional (2D) linearized Usadel equation

$$\xi_F^2 \left(\frac{\partial^2}{\partial x^2} + \frac{\partial^2}{\partial y^2} \right) \Theta_F - \frac{\tilde{\omega}}{\pi T_c} \Theta_F = 0, \tag{1}$$

where ω is the Matsubara frequency, $\tilde{\omega} = |\omega| + iE \operatorname{sign}(\omega)$, E is the exchange magnetic energy of the ferromagnetic material, its coherence length $\xi_F = (D_F / 2\pi T_c)^{1/2}$, and D_F is the electron diffusion coefficient. $\Theta_F = \Theta_F(x, y, \omega)$ is the parameterized Usadel function introduced by the expression $\Theta_F = \tilde{\omega} F_F / G_F$, where F_F and G_F are Usadel functions for the ferromagnetic region. We use the units where the Plank and Boltzmann constants are $\hbar = 1$ and $k_B = 1$. Under the assumption $|\gamma_{B1} - \gamma_{B2}| / \gamma_{B1}\gamma_{B2} \ll 1$ the boundary conditions at the FS interfaces located at $x = d_F$ can be written in the form[30]

$$\gamma_{B1} \frac{\xi_F}{\tilde{\omega}} \frac{\partial}{\partial x} \Theta_F = \frac{\Delta \exp\left(i \frac{\varphi}{2} \right)}{\sqrt{\omega^2 + \Delta^2}}, \quad 0 \le y \le \frac{L}{2},$$

$$\gamma_{B2} \frac{\xi_F}{\tilde{\omega}} \frac{\partial}{\partial x} \Theta_F = \frac{\Delta \exp\left(i \frac{\varphi}{2} \right)}{\sqrt{\omega^2 + \Delta^2}}, \quad \frac{L}{2} \le y \le L. \tag{2}$$

Here Δ is the modulus of the order parameter of the superconducting electrodes, and the phase of the order parameter takes the values $\pm\varphi/2$ on the two junction sides, respectively. These conditions directly follow from Kupriyanov-Lukichev boundary conditions (see Ref. 30) in the case of small transparent interface and had been intensively used for analysis of a wide scope of problems in SF multilayers with small transparent interfaces.[1–3] The boundary condition at the interface covered by the insulating film ($x = 0$) is[30]

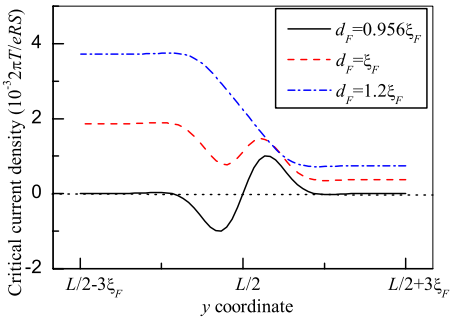

FIG. 2. (Color online) Critical current-density distribution (in units of $\pi T/eRS$) along the nonuniform SIFS Josephson junction. The temperature is $T=0.1T_c$, the exchange magnetic energy is $E=35\pi T_c$. $\gamma_{B1}=2$ and $\gamma_{B2}=10$. $d_F=0.956\xi_F$ corresponds to the point of the 0-π transition; for $d_F=1.2\xi_F$ the junction is far from the transition.

$$\frac{\partial}{\partial x}\Theta_F = 0. \tag{3}$$

At the free ends of the junction located at $y=0,L$ the boundary conditions correspond to zero current through these surfaces and have the form

$$\frac{\partial}{\partial y}\Theta_F = 0. \tag{4}$$

The final expressions for the solution of this two-dimensional boundary problem $\Theta_F(x,y,\omega)$ are presented in the Appendix [Eq. (A1)]. The Usadel function $\Theta_F(x,y,\omega)$ is substituted into the expression for the superconducting tunnel current density,[31] which gives the sinusoidal current-phase dependence $J(\varphi)=J_C(y)\sin(\varphi)$ with the critical current-density distribution of the following form

$$J_C(y) = \frac{2\pi T}{eRS}\sum_{\omega=0}^{\infty}\frac{\Delta}{\sqrt{\Delta^2+\omega^2}}\mathrm{Re}\left[\frac{\Theta_F(0,y,\omega)}{\tilde{\omega}}\right], \tag{5}$$

where R is the normal resistance of the tunnel SIFS junction. The calculation of $J_C(y)$ yields the following unexpected result: at some parameters [for example, the ferromagnet thickness d_F (Ref. 32)] when the uniform junction is close to a 0-π transition ($J_C=0$), $J_C(y)$ [Eq. (5)] exhibits damped oscillations in the vicinity of the transparency step (Fig. 2). $J_C(y)$ changes sign so that the junction properties change from the 0 state to the π state on the scale of ξ_F. This means that a 0-π nanojunction with zero total critical current is formed inside the structure. Previously, a similar effect was predicted for a SFIFS-SNINS nonuniform junction.[33] Note that we call "0-π transition" the conditions when the uniform junction has zero critical current, and "0-π nanojunction" the region where the critical current density is nonuniform and changes its sign near the junction nonuniformity under these conditions.

B. Maximum Josephson current in an external magnetic field

The nonuniform distribution of the critical current density must lead to some peculiarities in the junction behavior in an external magnetic field. We start from the Ferrell-Prange-type equation for an inhomogeneous Josephson junction

$$\lambda_J^2\frac{\partial^2}{\partial y^2}\varphi(y) - \frac{J_C(y)}{J_{C0}}\sin\varphi(y) = \frac{J}{J_{C0}}. \tag{6}$$

Here

$$\lambda_J = \sqrt{\frac{\Phi_0}{2\pi d_L J_{C0}\mu_0}} \tag{7}$$

is the Josephson penetration depth, where J_{C0} is the maximum of the critical current density along the junction, J is the bias current density, $d_L=d_F+d_I+2\lambda_L$, and λ_L is the London penetration depth of S regions. We assume that the ferromagnetic layer is thin enough to neglect its influence on λ_L.

Since the typical scale of the critical current oscillations is $\xi_F \ll \lambda_J$, it is more interesting to examine a Josephson junction of intermediate length L in the y direction: $\xi_F, \lambda_L \ll L \ll \lambda_J$. It is also assumed that the width of the junction in the z direction exceeds the value λ_L. Under these conditions it is possible to use the local Eq. (6).[34] In this case the solution of Eq. (6) can be found in the linear form $\varphi(y)=\varphi_0+hy/\xi_F$, where $h=H/H_0$ is the normalized applied magnetic field in the z direction, and $H_0=\Phi_0/2\pi\mu_0\xi_F d_L$.

The total current through the junction is calculated and the phase difference φ_0 providing the maximum of the total current at each value of h is determined. This yields the dependence of the maximum Josephson current through the junction on the external magnetic field $I_{\max}(H)$, which is given in the Appendix [Eq. (A2)].

If the ferromagnet thickness d_F has a value such that the JJ is either in the 0 or π state, then $I_{\max}(H)$ is mainly defined by the first term under the square root in the expression Eq. (A2). This term describes the contribution of the average critical current density along the junction. The corresponding dependence $I_{\max}(H)$ resembles a Fraunhofer pattern that is typical for uniform Josephson junctions. With increasing nonuniformity $\gamma_{B2}/\gamma_{B1}\neq 1$ the oscillation period of the Fraunhofer-type pattern is doubled [compare the dash-dotted and the dash-dotted-dotted lines in Fig. 3(a)]. From the calculation of the current distribution, we find that this is due to the fact that only one half of the junction actually conducts the current in this situation.

If the junction approaches the point of the 0-π transition, the 0-π nanojunction forms inside the structure and the picture changes by the following way: the maximum Josephson current goes up if the magnetic flux through the JJ $\Phi=HS$ increases first keeping its oscillations [Fig. 3(a)]. This increase continues up to a very large magnetic flux. When the Fraunhofer oscillations have a period of Φ_0, the correspondent flux has a much larger scale [Fig. 3(b)]. $I_{\max}(\Phi)$ achieves its maximum value when the magnetic flux through the nanojunction $\Phi'/\Phi_0=1$. Φ' depends on the length of the nanojunction that is defined by the critical current nonuniformity region $\sim\xi_F$, and does not depend on L. The magnetic flux Φ through the whole junction giving the maximum of $I_{\max}(\Phi)$ depends on the ratio L/ξ_F. The physics of this effect is rather transparent. The external field destroys the initial

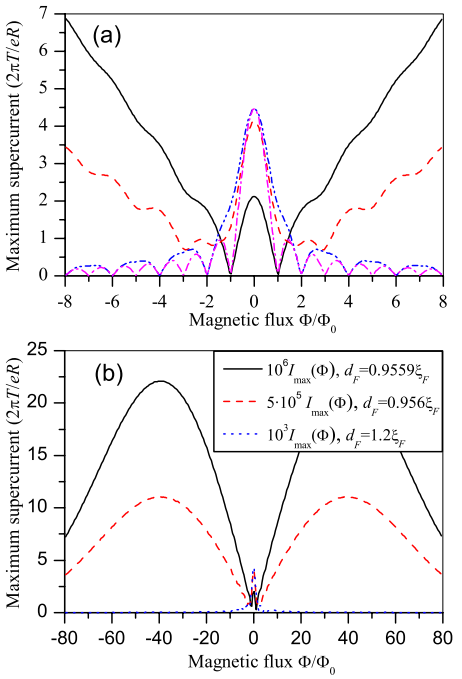

FIG. 3. (Color online) Maximum total supercurrent (in units of $2\pi T/eR$) of an SIFS JJ as a function of the magnetic flux through the junction (in units of Φ_0) for different ferromagnetic layer thicknesses d_F (the 0-π transition is at $d_F=0.9559\xi_F$). The junction length is $L=50\xi_F$, the temperature is $T=0.1T_c$, the exchange magnetic energy is $E=35\pi T_c$. $\gamma_{B1}=2$ and $\gamma_{B2}=10$. Panel (a) also includes the Fraunhofer pattern (dash-dotted line) for the homogeneous JJ ($\gamma_{B1}=\gamma_{B2}=6$). Panel (b) shows the same dependencies on a larger magnetic-field scale.

antisymmetric distribution of the supercurrent inside the nanojunction (Fig. 2). Since the external field increases, the antisymmetry vanishes, and the full current across the junction grows. A similar $I_{\max}(\Phi)$ dependence with a minimum current at zero field was obtained experimentally and described theoretically for 0-π JJs with a step in the F layer thickness.[9,10,12] In our case the extraordinary high value of the field is related to the very small size of the nanojunction $\sim\xi_F$.

To fabricate such structures one needs the junction to be close to the 0-π transition (d_F close to $d_F^{0\text{-}\pi}$) with high precision. Since $d_F^{0\text{-}\pi}$ depends on T this could be realized by changing T, as temperature-induced 0-π transitions in SFS JJs were already observed.[9,35,36]

To enhance this effect one can create a periodic array of 0-π nanojunctions. The influence of the nanojunctions would be most significant if the length of every step is comparable with the size $\sim\xi_F$ of $I_C(y)$ oscillations. This is difficult to realize technologically because the value of ξ_F is rather small ~1 nm. Moreover, it seems to be necessary to keep the layer thicknesses with very high precision along the entire array.

III. SIFNS AND SINFS STRUCTURES

A. Boundary problem

To overcome the difficulties mentioned above we have considered a junction with an additional normal-metal layer,

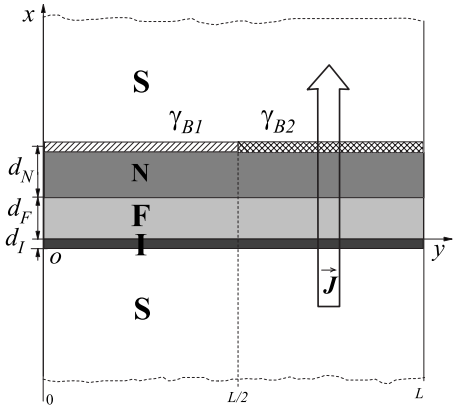

FIG. 4. Schematic view of a SIFNS Josephson junction with a steplike change in the NS interface transparency.

i.e., nonmagnetic ($E=0$) and nonsuperconducting ($\Delta=0$), with a thickness d_N (Fig. 4). The NS boundary has a steplike change in transparency. Now a nonuniform NS boundary is described by the suppression parameters γ_{B1} for $0\le y\le L/2$ and γ_{B2} for $L/2\le y\le L$, respectively, which are supposed to be large enough to neglect the suppression of superconductivity in the S electrode.

The corresponding boundary problem for the linearized Usadel equation differs from the previous one by the existence of the additional normal layer. Now the set of linearized Usadel equations includes also the equation for the N region that is written similarly to Eq. (1) as

$$\xi_N^2\left(\frac{\partial^2}{\partial x^2}+\frac{\partial^2}{\partial y^2}\right)\Theta_N-\frac{\omega}{\pi T_c}\Theta_N=0, \tag{8}$$

where the normal-metal coherence length $\xi_N=(D_N/2\pi T_c)^{1/2}$, and D_N is the diffusion coefficient. The boundary conditions for the nonuniform NS interface ($x=d_F+d_N$) have the form

$$\gamma_{B1}\xi_N\frac{\partial}{\partial x}\Theta_N=\frac{\omega\Delta\exp\left(i\frac{\varphi}{2}\right)}{\sqrt{\omega^2+\Delta^2}},\quad 0\le y\le\frac{L}{2}, \tag{9}$$

$$\gamma_{B2}\xi_N\frac{\partial}{\partial x}\Theta_N=\frac{\omega\Delta\exp\left(i\frac{\varphi}{2}\right)}{\sqrt{\omega^2+\Delta^2}},\quad \frac{L}{2}\le y\le L. \tag{10}$$

The boundary conditions at the FN surface located at $x=d_F$ can be written as

$$\frac{\xi_N}{|\omega|}\frac{\partial}{\partial x}\Theta_N=\gamma\frac{\xi_F}{\tilde{\omega}}\frac{\partial}{\partial x}\Theta_F, \tag{11}$$

$$\Theta_F+\gamma_B\xi_F\frac{\partial}{\partial x}\Theta_F=\frac{\tilde{\omega}}{|\omega|}\Theta_N,$$

$$\gamma_B=R_{BF}2S/\rho_F\xi_F,\quad \gamma=\rho_N\xi_N/\rho_F\xi_F, \tag{12}$$

where R_{BF} is the resistance of the FN interface; $\rho_{N(F)}$ is the resistivity of the N or F layer, respectively. There are also

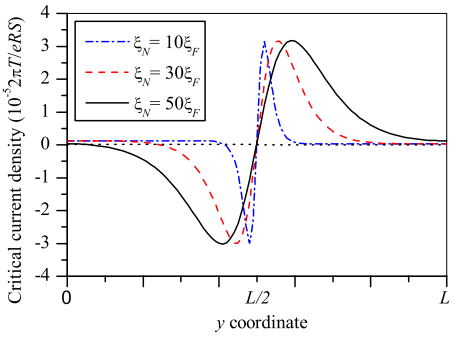

FIG. 5. (Color online) Critical current-density distribution (in units of $2\pi T/eRS$) along the nonuniform SIFNS Josephson junction of length $L=2000\xi_F$ at different N layer thicknesses d_N and ξ_N so that $d_N/\xi_N=5$. The temperature is $T=0.1T_c$, the exchange magnetic energy is $E=35\pi T_c$, the nonuniform NS boundary damping parameter is $\gamma_{B1}=2$, $\gamma_{B2}=10$, the FN boundary parameters are $\gamma=0.1$, $\gamma_B=0.2$, the ferromagnetic layer thickness $d_F=0.987\xi_F$ corresponds to the point of the 0-π transition.

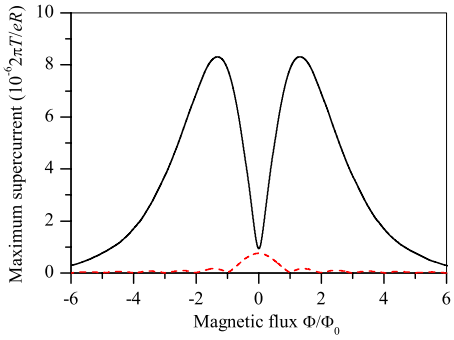

FIG. 6. (Color online) $I_{\max}(\Phi)$ (in units of $2\pi T/eR$) of a SIFNS JJ and its Fraunhofer part given by the first term under the square root of Eq. (A6) (dashed line). The conducting layer thicknesses are $d_F=0.987\xi_F$ and $d_N=5\xi_N$; $\xi_N=50\xi_F$, the junction length is $L=2000\xi_F$, the temperature is $T=0.1T_c$, the exchange magnetic energy is $E=35\pi T_c$, the nonuniform NS boundary damping parameter is $\gamma_{B1}=2$, $\gamma_{B2}=10$, and the FN boundary parameters are $\gamma=0.1$, $\gamma_B=0.2$.

additional conditions at the free interfaces of the N layer located at $y=0$ and $y=L$

$$\frac{\partial}{\partial y}\Theta_N = 0. \tag{13}$$

This boundary problem [Eqs. (1), (2), (4), and (8)–(13)] was solved analytically. The solution is presented in the Appendix [Eqs. (A3) and (A4)]. Inserting Eq. (A4) into the expression [Eq. (5)] it follows that $J_C(y)$ has changed in comparison to the SIFS junction, as can be seen in Fig. 5.

The current distribution keeps its form, but stretches along the y axis proportionally to ξ_N. The reason is an interplay of the ferromagnetic and the normal coherence lengths due to the proximity effect. The Usadel function in the N region noticeably changes on the distance of the order of ξ_N from the step at $y=L/2$. Subsequently, the ferromagnet "feels" this change also on the distance $\sim\xi_N$ from the step and conducts this information to the other superconducting electrode. The FN interface parameters γ and γ_B, and the ratio $s=\xi_N/\xi_F$ define the strength of this influence. This effect holds also when $d_N \ll \xi_N$. A thicker N layer slightly extends the length scale of the $J_C(y)$ oscillation, but also decreases the absolute value of J_C. The $J_C(y)$ distribution is shown in Fig. 5 for various values of d_N and s. While the d_N/s ratio stays constant, the 0-π transition occurs at the same conditions (d_F, T, γ, γ_B and so on).

Thus, the scale of the $J_C(y)$ changes in the y direction is $\propto\xi_N$ and can be hundreds times larger than ξ_F. It is a very interesting manifestation of the FN proximity effect that was already described for other geometries.[37–39] The critical current oscillation arises due to the presence of the ferromagnet in the structure, but the normal metal determines the period of J_C oscillations in the y direction. Thus, we have constructed a 0-π nanojunction on the scale of $\xi_N \gg \xi_F$.

B. SIFNS junction in an external magnetic field

It is clear that the size of the critical current nonuniformity influences the junction behavior in the external magnetic field. The dependence $I_{\max}(H)$ for the junction near the 0-π transition and $I_{\max}(H)$ for the uniform JJ with an average interface transparency are shown in Fig. 6. Here the 0-π nanojunction is wider than the one inside the SIFS junction, so that one needs much lower magnetic fields to destroy its asymmetry. Therefore, the width of the peaks becomes smaller and comparable to the Fraunhofer oscillation period when the junction length $L\sim\xi_N$. The detail of these calculations are presented in the Appendix.

It is also interesting to investigate a tunnel JJ with reversed order of the F and N layers, namely, a SINFS structure. The solution of the boundary problem is similar to Eqs. (1), (2), (4), and (8)–(13) for such a SINFS junction with the same NF boundary parameters γ, γ_B, and the same resistances R_{B1}, R_{B2} of the FS interface yield exactly the same expression [Eq. (A5)] for $J_C(y)$. This means that the Josephson effect and the magnetic properties of these nonuniform tunnel structures do not depend on the order of the F and N layers. The length scale of $J_C(y)$ oscillations is defined by the layer with the largest coherence length. This statement remains valid as long as one may use the linearized equations.

C. Microvortex forming

One can also consider the opposite problem, i.e., the influence of a direct current on the magnetic-field distribution inside the SIFNS structure. An interesting question is: can the 0-π nanojunction include some fractional Josephson vortex as in long 0-π Josephson junctions? Naturally in the ground state when the current through the JJ is equal to zero, $I=0$, the equilibrium phase distribution $\varphi(y)$ remains constant along the junction due to the small size of this nanojunction $\sim\xi_N \ll \lambda_J$, as λ_J is the typical length scale for the phase changes.

Let us consider the case when the current through the junction is finite, but does not exceed its maximum value, i.e., $0<I\leq I_{\max}$. Qualitatively, since one part of the nonuniform junction conducts the Josephson current much better than the other one (due to the difference in the NS boundary

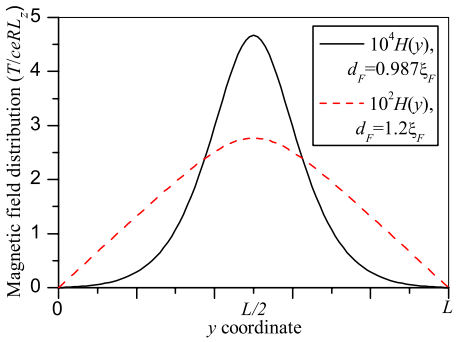

FIG. 7. (Color online) Magnetic-field distribution along a SIFNS junction at bias current $I=I_{\max}(0)$ for different thicknesses of the F layer. $d_F=0.987\xi_F$ corresponds to the point of the 0-π transition, with magnetic flux through the junction $\Phi_{0\text{-}\pi}=0.135\mu_0 d_L T/eR$; far from the 0-$\pi$ transition at $d_F=1.2\xi_N$, $\Phi=15.8\mu_0 d_L T/eR$. The N layer thickness is $d_N=5\xi_N$, $\xi_N=50\xi_F$, the junction length is $L=2000\xi_F$, the temperature is $T=0.1T_c$, the exchange magnetic energy is $E=35\pi T_c$, the nonuniform NS boundary damping parameter is $\gamma_{B1}=2$, $\gamma_{B2}=10$, and the FN boundary parameters are $\gamma=0.1$, $\gamma_B=0.2$.

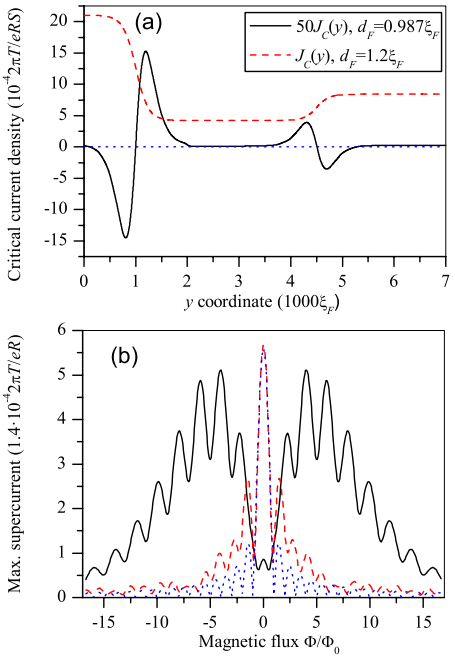

FIG. 8. (Color online) Asymmetric SIFNS Josephson junction having three regions with NS boundary damping parameters $\gamma_{B1}=2$, $\gamma_{B2}=10$, and $\gamma_{B3}=5$ and lengths $L_1=1000\xi_F$, $L_2=3500\xi_F$, and $L_3=2500\xi_F$, respectively. (a) $J_C(y)$ and (b) $I_{\max}(\Phi)$ in the vicinity of the 0-π transition ($d_F=0.987\xi_F$) and far from this transition ($d_F=1.2\xi_F$). Panel (b) also includes the Fraunhofer pattern (dash-dotted line) for the homogeneous JJ ($\gamma_{B1}=\gamma_{B2}=\gamma_{B3}=6$ and $d_F=1.2\xi_F$). The N layer thickness is $d_N=5\xi_N$, $\xi_N=50\xi_F$, the temperature is $T=0.1T_c$, the exchange magnetic energy is $E=35\pi T_c$, and the FN boundary parameters are $\gamma=0.1$, $\gamma_B=0.2$.

transparency and consequently in the value of J_C), the supercurrent redistributes within the junction area. This redistribution can be interpreted as a vortex of supercurrent. This vortex produces a magnetic field in the z direction and is pinned around $y=L/2$, where the transparency changes stepwise. The distribution of the magnetic field and the corresponding magnetic flux have been calculated under the assumption that the local phase variation is much smaller than its average value.

The largest magnetic flux is induced when the Josephson current takes its maximum value $I=I_{\max}$. Far from the 0-π transition the magnetic-field distribution increases almost linearly up to the nonuniformity point $y=L/2$ with a smooth extremum at $y=L/2$ as shown by the dashed line in Fig. 7. At the same time at $d_F=d_F^{0\text{-}\pi}$ the field distribution has a typical width (Fig. 7) comparable to the length of the critical current nonuniformity (see Fig. 5). The corresponding magnetic flux $\Phi_{0\text{-}\pi}$ in this case does not depend on the junction length L contrary to the case of the junction far from the 0-π transition. The value of $\Phi_{0\text{-}\pi}$ is smaller than Φ due to the small length of the nanojunction and small value of the critical current, i.e.,

$$\frac{\Phi}{\Phi_0} \sim \frac{L^2}{\lambda_J^2}\frac{|\gamma_{B1}-\gamma_{B2}|}{\gamma_{B1}+\gamma_{B2}}, \frac{\Phi_{0\text{-}\pi}}{\Phi_0} \sim \frac{\xi_N^2}{\lambda_J^2}\frac{|\gamma_{B1}-\gamma_{B2}|}{\gamma_{B1}+\gamma_{B2}}.$$

Here λ_J is defined by Eq. (7), with $d_L=d_N+d_F+d_I+2\lambda_L$.

IV. SIFNS JUNCTION WITH FEW STEPS OF BOUNDARY TRANSPARENCY

Technology does not allow fabricating ferromagnetic JJs with ideally smooth interfaces. Moreover, one often uses a thin normal layer below the ferromagnet to improve the JJ properties.[11,36] The interlayer boundary nonuniformity may create peculiarities in the $J_C(y)$ distribution that have an effect on the junction behavior in an external magnetic field. In order to describe this behavior, as a first attempt it would be reasonable to consider a SINFS Josephson junction having a few steps of the boundary transparency. At first, we take three steps with different lengths and FS boundary damping parameters γ_{B1}, γ_{B2}, and γ_{B3}, respectively. The length L_i of every step is assumed to be $L_i \geq \xi_N$, but the length of the whole junction remains $L \ll \lambda_J$. Under these assumptions the function $J_C(y)=J_{Ci}$ becomes a constant far enough from the nonuniformities (J_{Ci} is the critical current density of the uniform JJ with the damping parameter γ_i). In this region the condition $\partial J_C(y)/\partial y=0$ is fulfilled as on a free end of the junction. Therefore, the solution of the corresponding boundary problem may be constructed from the solutions presented above

$$J_C(y) = J_C(y, \gamma_{B1}, \gamma_{B2}), \text{ if } 0 \leq y \leq 2L_1,$$

$$J_C(y) = J_C(y, \gamma_{B2}, \gamma_{B3}), \text{ if } 2L_1 \leq y \leq 2L_1 + 2L_3,$$

where $L_2=L_1+L_3$.

$J_C(y)$ at $d_F=d_F^{0\text{-}\pi}$ is neither symmetric, nor antisymmetric in the y direction, see Fig. 8(a). Such a distribution $J_C(y)$ results in a rather complicated $J_{\max}(H)$ dependence, which remains non-Fraunhofer far from the 0-π transition, see Fig. 8(b).

If the junction is symmetric $\gamma_{B1}=\gamma_{B3}$ and $L_1=L_2/2=L_3$, there are two different situations $\gamma_{B1}=\gamma_{B3}<\gamma_{B2}$ and γ_{B1}

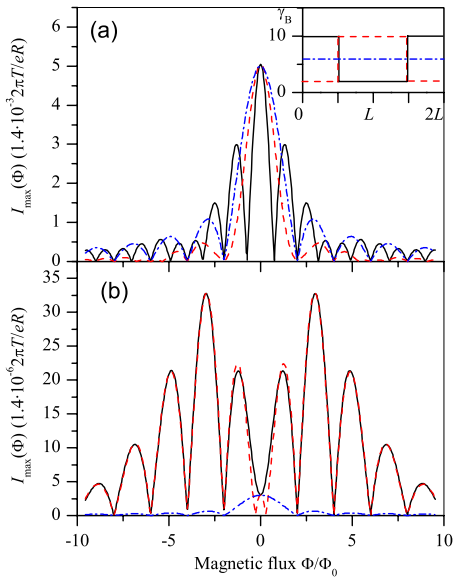

FIG. 9. (Color online) $I_{max}(\Phi)$ of the symmetric SIFNS Josephson junction having three regions of the NS boundary transparency (a) far from the 0-π transition $d_F=1.2\xi_F$, and (b) in the vicinity of the transition $d_F=0.987\xi_F$. NS interface damping parameters $\gamma_{B1}=\gamma_{B3}$ and γ_{B2} take the values 2 and 10, as it is shown in the inset. $L_1=L_3=L_2/2$, $L_1+L_2+L_3=L=3500\xi_F$. The N layer thickness is $d_N=5\xi_N$, $\xi_N=50\xi_F$, the temperature is $T=0.1T_c$, the exchange magnetic energy is $E=35\pi T_c$, and the FN boundary parameters are $\gamma=0.1$, $\gamma_B=0.2$.

$=\gamma_{B3}>\gamma_{B2}$. The first one corresponds to one junction with a large J_C in the center of the structure, and the second one is two junctions with a large J_C of twice less length near its ends. Therefore, far from the 0-π transition the period of the $I_{max}(H)$ dependence will be twice smaller than in the first case [Fig. 9(a)]. In the vicinity of the 0-π transition the picture is practically the same for both cases, see Fig. 9(b). The reason is that in this situation the Josephson current is defined mainly by two 0-π nanojunctions related to oscillations of $J_C(y)$ in the nonuniformity areas.

Such a consideration could help to understand how the interlayer roughness or nonuniformity of the interfaces (of length $\sim\xi_N$) leads to deviations in $I_{max}(H)$ from the Fraunhofer pattern obtained for the uniform structure with the averaged parameters. This deviation would depend not only on the value of the roughness but also on its distribution in the junction plane.

V. SIFNS JUNCTIONS ARRAY

A. JJ arrays in a magnetic field

The relatively long range of $J_C(y)$ nonuniformity in the SIFNS structure makes it possible to fabricate an array of nanojunctions with periodic steplike changes in the transparency of the NS interface. The transparency step must be sharp in comparison with ξ_N and it is assumed that the length L_i of every uniform part satisfies the conditions: $\xi_N<L_i\ll\lambda_J$.

Obviously the periodic oscillation of the transparency leads to variations in the Usadel functions Θ_N and Θ_F and

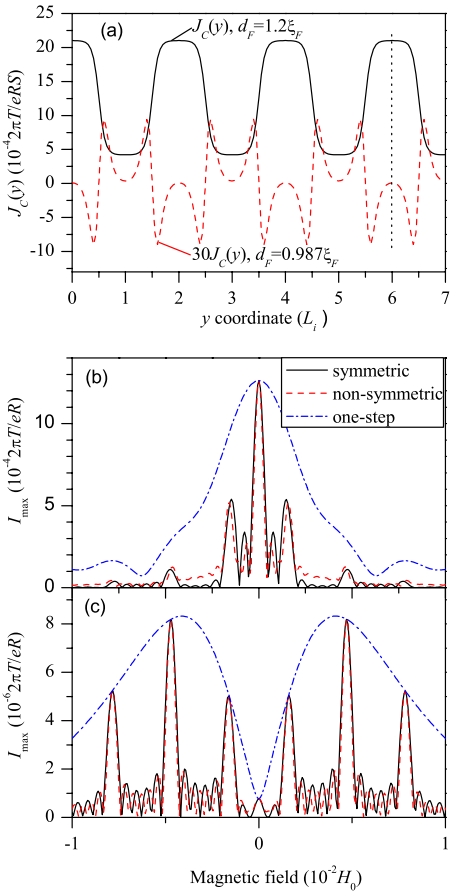

FIG. 10. (Color online) SIFNS JJ with periodically changing damping parameter of the NS boundary between $\gamma_{B1}=2$ and $\gamma_{B2}=10$. (a) $J_C(y)$, (b) $J_{max}(H)$ for a JJ far from the 0-π transition ($d_F=1.2\xi_F$), and (c) in the vicinity of the 0-π transition ($d_F=0.987\xi_F$). The N layer thickness is $d_N=5\xi_N$, $\xi_N=50\xi_F$, the temperature is $T=0.1T_c$, the exchange magnetic energy is $E=35\pi T_c$, and the FN boundary parameters are $\gamma=0.1$, $\gamma_B=0.2$, and $L_i=2000\xi_F$. The length of the symmetric junction $L=6L_i$ is indicated on plot (a) by the dashed line. The dependence $I_{max}(H)$ for the junction with only one NS boundary transparency step is shown on (b) and (c) for comparison.

the critical current density along the junction with the same period. The expression [Eqs. (A3) and (A4)] for $\Theta_{N,F}$ has a form of a series of $2L_i$ periodic functions. So, the expression for the function of the periodic array, where the NS boundary damping parameter takes the alternating values γ_{B1} and γ_{B2}, may be constructed again as a simple continuation of the function $\Theta_{N,F}$ [Eqs. (A3) and (A4)] along the whole array. It has been proven that this boundary problem does not have any other solution.

The $J_C(y)$ calculated from Eqs. (5) and (A5) for the periodic structure far from and near to the 0-π transition is presented in Fig. 10(a). The periodic array could be symmetric (contains an integer number of transparency periods) or not symmetric (contains a semi-integer number of transparency periods), but its length is assumed to be much shorter than λ_J. In the symmetric case the expression for the maximum Josephson current $I_{max}(H)$ has only the term with $\sin(\pi\Phi/\Phi_0)$ (Φ is the magnetic flux through whole the junc-

tion). The simple sine dependence [Eq. (A7)] leads to the value $\varphi_0 = \pm \pi/2$ at which the maximum supercurrent $I_{\max}$ is realized. This value does not depend on H and on the array length as in the case of a uniform junction having the well-known Fraunhofer $I_{\max}(H)$ dependence. However, the coefficient in front of $\sin(\pi\Phi/\Phi_0)$ depends on the magnetic field due to the nonuniformity of the structure. It leads to deviations from the Fraunhofer pattern both far and near the 0-π transition, as shown in Figs. 10(b) and 10(c).

If the structure is not symmetric, the expression $I_{\max}(H)$ [Eq. (A8)] looks like a non-Fraunhofer function for one step structure. Both the symmetric and nonsymmetric arrays give similar complicated curves $I_{\max}(H)$. The applied magnetic field together with nonuniform current distribution along the junction yield the appearance of additional oscillations and sharp peaks in the dependence $I_{\max}(H)$ [Figs. 10(b) and 10(c)].

The short oscillation period is defined by the magnetic flux through the whole array. The long period of the additional oscillations depends on the length of every step (i.e., the semiperiod of the structure nonuniformity), namely, on the value of the magnetic flux through this step. Near the 0-π transition the appearing sharp maxima lay under the envelope curve, which is nothing else but $I_{\max}(H)$ for a one step JJ of the same length. The distribution of the peaks heights (the third oscillation period) depends on the $J_C(y)$ nonuniformity scale, which is defined by the ratio ξ_N/ξ_F and the value of d_N.

The sharp peaks in $I_{\max}(H)$ arise not only in the vicinity of the 0-π transition, but also for an arbitrary ferromagnetic layer thickness. It means that it is not necessary to keep high precision of the parameters along the whole structure. These sharp peaks have obviously a similar origin as the periodic peaks on the voltage-field dependence of the periodic array of usual SIS JJs described in Refs. 23 and 25 The JJ with periodically changing interface transparency also can be considered as an array of large J_C junctions inserted between junctions with small J_C.

Now there are three scales: the length of the array L, the length of each region with constant transparency L_i, and the width of the critical current nonuniformity $\sim\xi_N$. All of them are assumed to be much smaller than λ_J. Their interplay defines the behavior of the structure in the external magnetic field and yields various unusual forms of the $I_{\max}(H)$ dependence. This allows designing the JJ arrays with peculiar magnetic properties.

B. Short-range oscillations averaging

Up to now it has been assumed that $L \ll \lambda_J$. If the junction length becomes comparable with λ_J (Refs. 10, 12, and 36) the linear phase ansatz cannot be used anymore. However, if the conditions $\xi_F, \xi_N \ll L_i \ll \lambda_J$ remain valid for each transparency region, one can select long-range ($\sim\lambda_J$) and short-range ($\sim L_i$) phase variations, and suppose that the short-range variations are much smaller than the long-range variations. Then the problem of calculation of the phase distribution along the nonuniform structure can be reduced to the well-known problem of a nonlinear oscillator behavior.[20,22] It was shown that the oscillating $J_C(y)$ leads to an effective second harmonic J_{C2} in the current-phase relation for the long-range (averaged) phase, i.e.,

$$J(\varphi) = J_{C1}\sin(\varphi) + J_{C2}\sin(2\varphi). \tag{14}$$

We have calculated the second harmonics J_{C2} for the SIFNS array with periodically changing transparency of the NS interface. The expression obtained by averaging out the short-range oscillations is presented in the Appendix [Eq. (A9)]. The second harmonic obtained in this way always has a negative value.

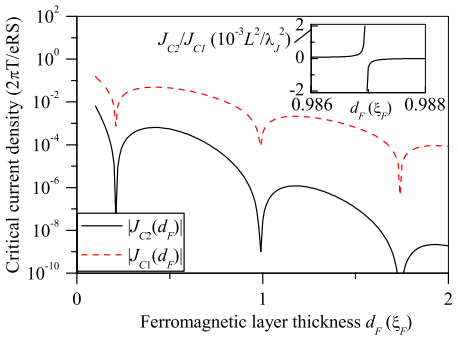

FIG. 11. (Color online) Effectively generated second harmonics in the current-phase relation in the comparison with the first harmonic for the JJ with periodically changing boundary transparency as a function of F layer thickness. The ratio J_{C2}/J_{C1} in a very small region ($0.986\xi_F < d_F < 0.988\xi_F$) near 0-$\pi$ transition (inset). NS boundary damping parameter takes in turn the values $\gamma_{B1}=2$ and $\gamma_{B2}=10$, the N layer thickness is $d_N=5\xi_N$, $\xi_N=50\xi_F$, the temperature is $T=0.1T_c$, the exchange magnetic energy is $E=35\pi T_c$, the FN boundary parameters are $\gamma=0.1$, $\gamma_B=0.2$, and the length of every homogeneous area is $L_i=2000\xi_F$.

The dependence of the first and the second harmonics vs d_F is presented in Fig. 11. The absolute value of J_{C2} is not large in comparison to J_{C1}. When the junction is far from the 0-π transition, J_{C2} increases and achieves its saturation as the length L_i increases. $J_C(y)$ does not change its sign along the junction, and the relation $|J_{C2}/J_{C1}| \sim L^2/2\pi\lambda_J^2$ is satisfied.

At $d_F \approx d_F^{0\text{-}\pi}$ where the junction is close to the 0-π transition and its first harmonics J_{C1} vanishes, the effective second harmonics J_{C2} is generated by the $J_C(y)$ nonuniformity. $J_C(y)$ changes its sign, but the regions where it occurs are too small (of the order of ξ_N, which defines the size of $J_C(y)$ nonuniformity area), so that $|J_{C2}/J_{C1}| \sim \xi_N^2/2\pi\lambda_J^2 \ll 1$. The ratio $|J_{C2}/J_{C1}|$ formally diverges at the 0-π transition point, see inset in Fig. 11. Thus, the question about the possibility of the so-called φ-junction realization arises here.

A φ junction is a JJ with the phase difference $\pm\varphi$ in the ground state ($0 < \varphi < \pi$). When in the JJ with current-phase relation [Eq. (14)] the conditions

$$\left|\frac{2J_{C2}}{J_{C1}}\right| > 1, \quad \text{and} \quad J_{C2} < 0 \tag{15}$$

are satisfied, the φ junction appears.[20,22,40]

φ-JJs can be used similar to π-JJs, but provide an arbitrary preprogrammed phase shift φ ($|\varphi| < \pi$). The φ junction has very interesting properties:[22,40] two critical currents, half-

integer zero-field steps that appear due to the motion of fractional Josephson vortices, half-integer Shapiro steps, and unusual Josephson current dependence on the external magnetic field and their behavior in the SQUID loop.

The vicinity of the 0-π transition could be achieved by the preparation of a high-quality junction with periodically changing interlayer boundary and changing of their temperatures. But the conditions [Eq. (15)] described above are difficult to achieve due to the very small value of the region where they are satisfied.

VI. CONCLUSIONS

In the framework of the microscopic model based on the linearized Usadel equations we have found that the steplike interface transparency inside the SIFS and SIFNS JJs leads to oscillations of the critical current density $J_C(y)$ along the junction, close to the 0-π transition ($d_F \approx d_F^{0\text{-}\pi}$). This, in turn, results in the formation of a nonuniform 0-π nanojunction with characteristic size of the order of ferromagnet coherence length ξ_F for the SIFS JJ. For the SIFNS or SINFS structures the nanojunction size is $\xi_N \gg \xi_F$.

The existence of this 0-π nanojunction inside the structure leads to an unusual dependence of maximum supercurrent $I_{\max}$ on the external magnetic field H. If the junction is close to the 0-π transition, i.e., in the regions $d_F \approx d_F^{0\text{-}\pi}$ so that $J_C(y) \to 0$, $|y - L/2| \geq \max\{\xi_F, \xi_N\}$, then the $I_{\max}(H)$ dependence is very different from the usual Fraunhofer pattern. $I_{\max}$ increases with H up to a certain value which may be very large. This value depends on the size of the nanojunction (ξ_N or ξ_F).

The reasonably large size ($\sim \xi_N$) of the 0-π nanojunction in the SIFNS structure makes it possible to fabricate a JJ with periodic steplike changes in the NS interface transparency. Such JJ may have additional oscillations and sharp peaks in $I_{\max}(H)$. Three relevant scales (the length of the array, the length of every region with constant transparency, and the length of the $I_C(y)$ nonuniformity) define three oscillation periods on $I_{\max}(H)$. These peculiarities are still present also far from the 0-π transition and this allows fabrication of these SQIF-like structures of a distinct type containing a ferromagnetic layer by modern technology.

ACKNOWLEDGMENTS

This work was supported by the Russian Foundation for Basic Research (Grants No. 08-02-90105-mol-a, No. 07-02-00918-a, and No. 09-02-12176-ofi-m), by the ENS-Landau program, by the Deutsche Forschungsgemeinschaft via Grant No. SFB/TRR21, and by the Deutscher Akademischer Austauschdienst.

APPENDIX

The parameterized Usadel function $\Theta_F(x, y, \omega)$ found as a solution of the boundary problem [Eqs. (1)–(4)] at the left part of the junction $0 \leq y \leq L/2$ can be written as

$$\Theta_F = \frac{\Delta\tilde{\omega}}{\sqrt{\Delta^2 + \omega^2}} \frac{\exp\left(i\frac{\varphi}{2}\right)}{\gamma_{B1}} \cdot \left\{ \frac{\cosh(\sqrt{\tilde{\omega}}x/\xi_F)}{\sqrt{\tilde{\omega}}\sinh(\sqrt{\tilde{\omega}}d/\xi_F)} - \frac{\gamma_{B2} - \gamma_{B1}}{\gamma_{B2}} d\xi_F \sum_{k=0}^{\infty}{}' \frac{(-1)^k \cos(\pi k x/d)}{d^2\tilde{\omega} + (\pi k \xi_F)^2} \times \exp\left[-\frac{|y - L/2|}{\xi_F} \sqrt{\tilde{\omega} + (\pi k \xi_F/d)^2} \right] \right\}, \quad \text{(A1)}$$

where Σ' means that at $k=0$ only half of the term is taken. The magnitude of order parameter and the Matsubara frequencies in Eq. (A1) and below are normalized on πT_c. The solution of the boundary problem [Eqs. (1)–(4)] at $L/2 \leq y \leq L$ can be reconstructed from Eq. (A1) by replacing γ_{B1} by γ_{B2}. The second term in Eq. (A1) describes the perturbation of the Usadel functions nucleated by changing of the FS interface transparency at $x = d_F$ and $y = L/2$. Substitution of Eq. (A1) into the standard expression for the Josephson current yields the $J_C(y)$ [Eq. (5)]. To find out the maximum Josephson current through the whole junction in the external magnetic field $I_{\max}(H)$, we start from the Ferrell-Prange-type equation for the nonuniform Josephson junction [Eq. (6)]. In the practically interesting limit $\xi_F \ll L \ll \lambda_J$, its solution $\varphi(y)$ can be found in the linear form. To calculate the maximum value of the supercurrent $\varphi(y)$ is substituted into Eq. (6) and Eq. (5) is integrated over y. Thus the obtained total supercurrent through the junction is further maximized with respect to phase difference φ_0. This procedure finally leads to

$$I_{\max}(h) = \frac{2\xi_F}{hL} \sqrt{[\Sigma_1 \sin(hL/2\xi_F)]^2 + [\Sigma_2(h)]^2}, \quad \text{(A2)}$$

where

$$\Sigma_1 = \frac{\gamma_{B1} + \gamma_{B2}}{\gamma_{B1}\gamma_{B2}} \frac{2\pi T}{eR} \sum_{\omega=0}^{\infty} \frac{\Delta^2}{\Delta^2 + \omega^2} \mathrm{Re} \frac{\sqrt{\tilde{\omega}}}{\sinh\left(\frac{d}{\xi_F}\sqrt{\tilde{\omega}}\right)},$$

$$\Sigma_2 = \frac{\gamma_{B2} - \gamma_{B1}}{\gamma_{B1}\gamma_{B2}} \frac{2\pi T}{eR} \sum_{\omega=0}^{\infty} \frac{\Delta^2\sqrt{\tilde{\omega}}}{\Delta^2 + \omega^2} \cdot \mathrm{Re}\left[\frac{1}{\sqrt{\tilde{\omega} + h^2}\sinh\left(\frac{d}{\xi_F}\sqrt{\tilde{\omega} + h^2}\right)} - \frac{\cos(hL/2\xi_F)}{\sqrt{\tilde{\omega}}\sinh\left(\frac{d}{\xi_F}\sqrt{\tilde{\omega}}\right)} \right].$$

The first term under the square root in the expression [Eq. (A2)] corresponds to the investment of uniform regions $|y - L/2| > \xi_F$ and has the Fraunhofer form, while the second term with Σ_2 contains more complicated dependence on h and describes the nonuniformity of $J_C(y)$ and it is connected to peculiarities of $I_{\max}(h)$. It exceeds the first term in the vicinity of the 0-π transition. It is clearly seen from Eq. (A2) that in the absence of the nonuniformity ($\gamma_{B1} = \gamma_{B2}$, thus $\Sigma_2 = 0$) the dependence of $I_{\max}(h)$ reduces to the well-known Fraunhofer pattern.

The boundary problem Eqs. (1), (2), (4), and (8)–(13) for the SIFNS junction has been solved analytically both for N and F layers. The derivatives on the free ends of the junction $\partial\Theta_{N,F}/\partial y=0$ at $y=0,L$ Eqs. (4) and (13), therefore, the solution in normal-metal layer is found in the form

$$\Theta_N(x,y,\omega)=\exp\left(i\frac{\varphi}{2}\right)\left\{A(x)+\sum_{n=0}^{\infty}A_n(x)\cos\left[\pi(2n+1)\frac{y}{L}\right]\right\}, \tag{A3}$$

where the coefficients

$$A(x)=a\cosh\left(\frac{x-d_F-d_N}{\mu}\right)+\frac{\mu}{2\xi_N}\frac{\Delta}{\sqrt{\omega^2+\Delta^2}}\frac{\gamma_{B1}+\gamma_{B2}}{\gamma_{B1}\gamma_{B2}}\sinh\left(\frac{x-d_F-d_N}{\mu}\right),$$

$$A_n(x)=a_n\cosh\left(\frac{x-d_F-d_N}{\mu_m}\right)-\frac{2(-1)^n\mu_n}{\pi(2n+1)\xi_N}\frac{\Delta}{\sqrt{\omega^2+\Delta^2}}\frac{\gamma_{B1}-\gamma_{B2}}{\gamma_{B1}\gamma_{B2}}\sinh\left(\frac{x-d_F-d_N}{\mu_n}\right),$$

where

$$\mu=\frac{\xi_N}{\sqrt{\omega}},\quad \mu_n=\frac{\xi_N}{\sqrt{\left[\frac{\xi_N}{L}\pi(2n+1)\right]^2+\omega}},\quad n=0,1,2\ldots,$$

$$a=\frac{\gamma_{B1}+\gamma_{B2}}{\gamma_{B1}\gamma_{B2}}\frac{\Delta}{\sqrt{\omega^2+\Delta^2}}\frac{\mu}{2\xi_N}\cdot\frac{\xi_N\zeta\cosh\left(\frac{d_N}{\mu}\right)\cosh\left(\frac{d_F}{\zeta}\right)+\xi_F\gamma\mu\sinh\left(\frac{d_N}{\mu}\right)\sinh\left(\frac{d_F}{\zeta}\right)+\gamma_B\xi_F\xi_N\cosh\left(\frac{d_N}{\mu}\right)\sinh\left(\frac{d_F}{\zeta}\right)}{\xi_F\mu\gamma\sinh\left(\frac{d_F}{\zeta}\right)\cosh\left(\frac{d_N}{\mu}\right)+\xi_N\zeta\sinh\left(\frac{d_N}{\mu}\right)\cosh\left(\frac{d_F}{\zeta}\right)+\gamma_B\xi_N\xi_F\sinh\left(\frac{d_N}{\mu}\right)\sinh\left(\frac{d_F}{\zeta}\right)},$$

$$a_n=-\frac{\gamma_{B1}-\gamma_{B2}}{\gamma_{B1}\gamma_{B2}}\frac{\Delta}{\sqrt{\omega^2+\Delta^2}}\frac{2\mu_n(-1)^n}{\pi\xi_N(2n+1)}\cdot\frac{\xi_N\zeta_n\cosh\left(\frac{d_N}{\mu_n}\right)\cosh\left(\frac{d_F}{\zeta_n}\right)+\xi_F\gamma\mu_n\sinh\left(\frac{d_N}{\mu_n}\right)\sinh\left(\frac{d_F}{\zeta n}\right)+\gamma_B\xi_F\xi_N\cosh\left(\frac{d_N}{\mu_n}\right)\sinh\left(\frac{d_F}{\zeta_n}\right)}{\xi_N\zeta_n\sinh\left(\frac{d_N}{\mu_n}\right)\cosh\left(\frac{d_F}{\zeta_n}\right)+\xi_F\gamma\mu_n\sinh\left(\frac{d_F}{\zeta_n}\right)\cosh\left(\frac{d_N}{\mu_n}\right)+\gamma_B\xi_N\xi_F\sinh\left(\frac{d_N}{\mu_n}\right)\sinh\left(\frac{d_F}{\zeta_n}\right)},$$

where the parameters corresponding to the ferromagnet

$$\zeta=\frac{\xi_F}{\sqrt{\tilde{\omega}}},\quad \zeta_n=\frac{\xi_F}{\sqrt{\left[\frac{\xi_F}{L}\pi(2n+1)\right]^2+\tilde{\omega}}},\quad n=0,1,2\ldots.$$

Taking into account the boundary conditions Eqs. (3) and (4) the solution for the ferromagnetic layer can be written as

$$\Theta_F(x,y,\omega)=\frac{\tilde{\omega}\Delta\exp\left(i\frac{\varphi}{2}\right)}{|\omega|\sqrt{\omega^2+\Delta^2}}\left\{\frac{\gamma_{B1}+\gamma_{B2}}{\gamma_{B1}\gamma_{B2}}b\cosh\left(\frac{x}{\zeta}\right)-\frac{\gamma_{B1}-\gamma_{B2}}{\gamma_{B1}\gamma_{B2}}\sum_{n=0}^{\infty}b_n\cosh\left(\frac{x}{\zeta_n}\right)\cos\left[\pi(2n+1)\frac{y}{L}\right]\right\},$$

$$b=\frac{\mu\zeta/2}{\zeta\xi_N\sinh\left(\frac{d_N}{\mu}\right)\cosh\left(\frac{d_F}{\zeta}\right)+\mu\gamma\xi_F\sinh\left(\frac{d_F}{\zeta}\right)\cosh\left(\frac{d_N}{\mu}\right)+\gamma_B\xi_N\xi_F\sinh\left(\frac{d_N}{\mu}\right)\sinh\left(\frac{d_F}{\zeta}\right)},$$

$$b_n=\frac{2(-1)^n}{\pi(2n+1)}\frac{\mu_n\zeta_n}{\zeta_n\xi_N\sinh\left(\frac{d_N}{\mu_n}\right)\cosh\left(\frac{d_F}{\zeta n}\right)+\gamma\mu_n\xi_F\cosh\left(\frac{d_N}{\mu_n}\right)\sinh\left(\frac{d_F}{\zeta n}\right)\gamma_B\xi_F\xi_N+\sinh\left(\frac{d_N}{\mu_n}\right)\sinh\left(\frac{d_F}{\zeta n}\right)}. \tag{A4}$$

The critical current density given by the expression [Eq. (5)] turns out as follows:

$$J_C(y) = \frac{2\pi T}{eRS}\sum_{\omega=0}^{\infty}\frac{\Delta^2}{(\Delta^2+\omega^2)|\omega|}\left\{\frac{\gamma_{B1}+\gamma_{B2}}{\gamma_{B1}\gamma_{B2}}\mathrm{Re}\, b - \frac{\gamma_{B1}-\gamma_{B2}}{\gamma_{B1}\gamma_{B2}}\mathrm{Re}\sum_{n=0}^{\infty} b_n \cos\left[\pi(2n+1)\frac{y}{L}\right]\right\}. \tag{A5}$$

Substituting the solution $\varphi(y)$ in the linear form into the Ferrell-Prange [Eq. (6)], calculating the total current through the junction and maximizing it over φ_0, we arrive at the following $I_{\max}(h)$ dependence

$$I_{\max}(h) = \frac{2\xi_F}{hL}\sqrt{B_0^2\sin^2\left(\frac{hL}{2\xi_F}\right) + B_1^2(h)\cos^2\left(\frac{hL}{2\xi_F}\right)}, \tag{A6}$$

where

$$B_0 = \frac{\gamma_{B1}+\gamma_{B2}}{\gamma_{B1}\gamma_{B2}}\frac{2\pi T}{eR}\sum_{\omega=0}^{\infty}\frac{\Delta^2}{\Delta^2+\omega^2}\mathrm{Re}\frac{\sqrt{\tilde{\omega}}}{\sinh\left(\frac{d}{\xi_F}\sqrt{\tilde{\omega}}\right)}b,$$

$$B_1(h) = \frac{\gamma_{B2}-\gamma_{B1}}{\gamma_{B1}\gamma_{B2}}\frac{2\pi T}{eR}\sum_{\omega=0}^{\infty}\frac{\Delta^2}{\Delta^2+\omega^2}\sum_{n=0}^{\infty}\frac{\mathrm{Re}\, b_n}{\left[\frac{\pi(2n+1)\xi_F}{hL}\right]^2-1}.$$

Here B_0 describes the Fraunhofer contribution of the average $J_C(y)$, and B_1 corresponds to a non-Fraunhofer deviation due to the junction nonuniformity. The value $hL/2\xi_F=\pi\Phi/\Phi_0$ corresponds to the value of the magnetic flux Φ through the junction expressed in the units of magnetic-flux quantum Φ_0.

Let us consider an array with a periodic variation in the boundary resistivity. The junction contains M regions where the resistivity steplike changes and $M+1$ areas, where it is a constant, taking two alternating values R_1 and R_2. The uniform areas into the junction have the length L_i each, and $L_i/2$ on the ends. The boundary problem has the same periodic solution described by the expressions [Eqs. (A3) and (A4)]. The corresponding $J_C(y)$ is presented in Fig. 10(a). It yields the dependence $I_{\max}(H)$ for symmetric array $M=2N$, (N is an integer)

$$I_{\max}(h) = \frac{1}{f_s}\sin(f_s)|B_0 + B_2(h)|, \tag{A7}$$

here $f_s=M|h|L_i/2\xi_F=N|h|L_i/\xi_F=\pi\Phi/\Phi_0$ and

$$B_2(h) = \frac{\gamma_{B2}-\gamma_{B1}}{\gamma_{B1}\gamma_{B2}}\frac{2\pi T}{eR}\sum_{\omega=0}^{\infty}\frac{\Delta^2}{\Delta^2+\omega^2}\sum_{n=0}^{\infty}\frac{(-1)^{N+1}\mathrm{Re}\, b_n}{\left[\frac{\pi(2n+1)\xi_F}{hL_i}\right]^2-1}.$$

The term $\sin(f_s)/f_s$ coincides with the Fraunhofer dependence, but the function $B_2(h)$ makes $I_{\max}(H)$ dependence more complicated.

For a nonsymmetric array containing $M=2N+1$ nonuniformities [see the corresponding $J_C(y)$ in Fig. 10(a)], the nonsymmetric $J_C(y)$ yields the non-Fraunhofer pattern

$$I_{\max}(h) = \frac{1}{f_a}\sqrt{B_0^2\sin^2 f_a + B_2^2(h)\cos^2 f_a}, \tag{A8}$$

now

$$f_a = (2N+1)|h|L_i/2\xi_F = \pi\Phi/\Phi_0.$$

The dependencies [Eqs. (A7) and (A8)] have similar forms with an additional oscillation period connected to the magnetic flux through every uniform part of the structure $|h|L_i/\xi_F$, while the main (the shorter) period depends on the value $f_{s,a}=\pi\Phi/\Phi_0$. When $|h|=(2n+1)\pi\xi_F/L_i$ one of the terms of the sum $B_2(h)$ goes to infinity. It is not a real divergence but uncertainty of the type $\sin(x)/x$ at $x\to 0$. It gives a sharp maximum on the curve $I_{\max}(H)$, see Figs. 10(b) and 10(c).

If the structure becomes long enough, its length compares to the Josephson penetration depth λ_J but the length of each part remains $L_i \ll \lambda_J$, the linear approximation for the phase $\varphi(y)$ is impossible to use. Then it is necessary to solve the sine-Gordon [Eq. (6)].[40] It was shown[20,22] that a second harmonic in the current-phase relation [Eq. (14)] for the long-range phase effectively generates in this situation. The first harmonic in the SIFNS array is the average critical current $J_{C1}=B_0/S$. The expression for the effective second harmonic obtained by the averaging procedure described in Refs. 20 and 22 has the form

$$J_{C2} = -\frac{L_i^2}{4\pi^2\lambda_J^2|J_{C0}|}\sum_{n=0}^{\infty}\frac{B_n^2}{(2n+1)}, \tag{A9}$$

where

$$B_n = \frac{\gamma_{B2}-\gamma_{B1}}{\gamma_{B1}\gamma_{B2}}\frac{2\pi T}{eRS}\sum_{\omega=0}^{\infty}\frac{\Delta^2}{\Delta^2+\omega^2}\mathrm{Re}\, b_n. \tag{A10}$$

It is necessary to note that the product $\lambda_J^2|J_{C0}|$ does not depend on the value J_{C0}: $\lambda_J^2|J_{C0}|=\Phi_0/2\pi\mu_0(d_F+d_N+d_I+2\lambda_L)$ in accordance with the definition of λ_J. The dependence of the effective first and second harmonic of d_F is presented in Fig. 11.

*pugach@magn.ru

[1] A. I. Buzdin, Rev. Mod. Phys. **77**, 935 (2005).
[2] A. A. Golubov, M. Yu. Kupriyanov, and E. Il'ichev, Rev. Mod. Phys. **76**, 411 (2004).
[3] F. S. Bergeret, A. F. Volkov, and K. B. Efetov, Rev. Mod. Phys. **77**, 1321 (2005).
[4] L. B. Ioffe, V. B. Geshkenbein, M. V. Feigel'man, A. L. Fauchère, and G. Blatter, Nature (London) **398**, 679 (1999).
[5] T. Ortlepp, Ariando, O. Mielke, C. J. M. Verwijs, K. F. K. Foo, H. Rogalla, F. H. Uhlmann, and H. Hilgenkamp, Science **312**,

1495 (2006).
[6] E. Terzioglu, D. Gupta, and M. R. Beasley, IEEE Trans. Appl. Supercond. **7**, 3642 (1997).
[7] L. N. Bulaevskii, V. V. Kuzii, and A. A. Sobyanin, Solid State Commun. **25**, 1053 (1978).
[8] M. L. Della Rocca, M. Aprili, T. Kontos, A. Gomez, and P. Spathis, Phys. Rev. Lett. **94**, 197003 (2005).
[9] S. M. Frolov, D. J. Van Harlingen, V. V. Bolginov, V. A. Oboznov, and V. V. Ryazanov, Phys. Rev. B **74**, 020503(R) (2006).
[10] M. Weides, M. Kemmler, H. Kohlstedt, R. Waser, D. Koelle, R. Kleiner, and E. Goldobin, Phys. Rev. Lett. **97**, 247001 (2006).
[11] M. Weides, H. Kohlstedt, R. Waser, M. Kemmler, J. Pfeiffer, D. Koelle, R. Kleiner, and E. Goldobin, Appl. Phys. A: Mater. Sci. Process. **89**, 613 (2007).
[12] J. Pfeiffer, M. Kemmler, D. Koelle, R. Kleiner, E. Goldobin, M. Weides, A. K. Feofanov, J. Lisenfeld, and A. V. Ustinov, Phys. Rev. B **77**, 214506 (2008).
[13] J. H. Xu, J. H. Miller, Jr., and C. S. Ting, Phys. Rev. B **51**, 11958 (1995).
[14] E. Goldobin, D. Koelle, and R. Kleiner, Phys. Rev. B **66**, 100508(R) (2002).
[15] J. R. Kirtley, K. A. Moler, and D. J. Scalapino, Phys. Rev. B **56**, 886 (1997).
[16] T. Kato and M. Imada, J. Phys. Soc. Jpn. **66**, 1445 (1997).
[17] E. Goldobin, D. Koelle, and R. Kleiner, Phys. Rev. B **70**, 174519 (2004).
[18] E. Goldobin, D. Koelle, and R. Kleiner, Phys. Rev. B **67**, 224515 (2003).
[19] E. Goldobin, K. Vogel, O. Crasser, R. Walser, W. P. Schleich, D. Koelle, and R. Kleiner, Phys. Rev. B **72**, 054527 (2005).
[20] R. G. Mints, Phys. Rev. B **57**, R3221 (1998).
[21] R. G. Mints, I. Papiashvili, J. R. Kirtley, H. Hilgenkamp, G. Hammerl, and J. Mannhart, Phys. Rev. Lett. **89**, 067004 (2002).
[22] A. I. Buzdin and A. E. Koshelev, Phys. Rev. B **67**, 220504(R) (2003).
[23] J. Oppenländer, Ch. Häussler, and N. Schopohl, Phys. Rev. B **63**, 024511 (2000).
[24] J. Oppenländer, T. Träuble, Ch. Häussler, and N. Schopohl, IEEE Trans. Appl. Supercond. **11**, 1271 (2001).
[25] Ch. Häussler, J. Oppenländer, and N. Schopohl, J. Appl. Phys. **89**, 1875 (2001).
[26] V. Schultze, R. Ijsselsteijn, and H.-G. Meyer, Supercond. Sci. Technol. **19**, S411 (2006).
[27] V. K. Kornev, I. I. Soloviev, N. V. Klenov, and O. A. Mukhanov, Supercond. Sci. Technol. **19**, S390 (2006).
[28] A. Gumann, C. Inotakis, and N. Schopohl, Appl. Phys. Lett. **91**, 192502 (2007).
[29] M. Yu. Kupriyanov, N. G. Pugach, M. M. Khapaev, A. V. Vedyayev, E. B. Goldobin, D. Koelle, and R. Kleiner, Pis'ma Zh. Eksp. Teor. Fiz. **88**, 50 (2008) [JETP Lett. **88**, 45 (2008)].
[30] M. Yu. Kuprianov and V. F. Lukichev, Zh. Eksp. Teor. Fiz. **94**, 139 (1988) [Sov. Phys. JETP. **67**, 1163 (1988)].
[31] V. Ambegaokar and A. Baratoff, Phys. Rev. Lett. **10**, 486 (1963).
[32] A. S. Vasenko, A. A. Golubov, M. Yu. Kupriyanov, and M. Weides, Phys. Rev. B **77**, 134507 (2008).
[33] M. Yu. Kupriyanov, A. A. Golubov, and M. Siegel, *Nanoscale Devices–Fundamentals and Applications* (Springer, New York, 2006), p. 173.
[34] A. A. Abdumalikov, Jr, G. L. Alfimov, and A. S. Malishevskii, Supercond. Sci. Technol. **22**, 023001 (2009).
[35] V. A. Oboznov, V. V. Bolginov, A. K. Feofanov, V. V. Ryazanov, and A. I. Buzdin, Phys. Rev. Lett. **96**, 197003 (2006).
[36] M. Weides, M. Kemmler, E. Goldobin, D. Koelle, R. Kleiner, H. Kohlstedt, and A. Buzdin, Appl. Phys. Lett. **89**, 122511 (2006).
[37] T. Yu. Karminskaya and M. Yu. Kupriyanov, JETP Lett. **85**, 286 (2007) [Pis'ma Zh. Eksp. Teor. Fiz. **85**, 343 (2007)].
[38] T. Yu. Karminskaya and M. Yu. Kupriyanov, JETP Lett. **86**, 61 (2007) [Pis'ma Zh. Eksp. Teor. Fiz. **86**, 65 (2007)].
[39] T. Yu. Karminskaya, M. Yu. Kupriyanov, and A. A. Golubov, JETP Lett. **87**, 570 (2008) [Pis'ma Zh. Eksp. Teor. Fiz. **87**, 657 (2008)].
[40] E. Goldobin, D. Koelle, R. Kleiner, and A. Buzdin, Phys. Rev. B **76**, 224523 (2007).